Insertion of *Myc* into *Igh* Accelerates Peritoneal Plasmacytomas in Mice

Sung Sup Park,[1] Arthur L. Shaffer,[2] Joong Su Kim,[1] Wendy duBois,[1] Michael Potter,[1] Louis M. Staudt,[2] and Siegfried Janz[1]

[1]Laboratory of Genetics and [2]Metabolism Branch, Center for Cancer Research, National Cancer Institute, NIH, Bethesda, Maryland

Abstract

Gene-targeted mice that contain a His^6-tagged mouse c-*Myc* cDNA, Myc^{His}, inserted head to head into different sites of the mouse immunoglobulin heavy-chain locus, *Igh*, mimic the chromosomal T(12;15)(*Igh-Myc*) translocation that results in the activation of *Myc* in the great majority of mouse plasmacytomas. Mice carrying Myc^{His} just 5′ of the intronic heavy-chain enhancer Eμ (strain $iMyc^{E\mu}$) provide a specific model of the type of T(12;15) found in a subset (~20%) of plasmacytomas that develop "spontaneously" in the gut-associated lymphoid tissue (GALT) of interleukin-6 transgenic BALB/c (C) mice. Here we show that the transfer of the $iMyc^{E\mu}$ transgene from a mixed genetic background of segregating *C57BL/6* × *129/SvJ* alleles to the background of C increased the incidence of GALT plasmacytomas by a factor of 2.5 in first-generation backcross mice ($C.iMyc^{E\mu}$ N_1). Third-generation backcross mice ($C.iMyc^{E\mu}$ N_3, ~94% C alleles) were hypersusceptible to inflammation-induced peritoneal plasmacytomas (tumor incidence, 100%; mean tumor onset, 86 ± 28 days) compared with inbred C mice (tumor incidence, 5% on day 150 after tumor induction). Peritoneal plasmacytomas of $C.iMyc^{E\mu}$ N_3 mice overexpressed Myc^{His}, produced monoclonal immunoglobulin, and exhibited a unique plasma cell signature upon gene expression profiling on mouse Lymphochip cDNA microarrays. These findings indicated that the $iMyc^{E\mu}$ transgene accelerates plasmacytoma development by collaborating with tumor susceptibility alleles of strain C and circumventing the requirement for tumor precursors to acquire deregulated *Myc* by chromosomal translocation. (Cancer Res 2005; 65(17): 7644-52)

Introduction

Peritoneal plasmacytomagenesis in mice provides a model system for the study of inflammation-dependent cancer arising in terminally differentiated B lymphocytes, plasma cells (1). Unlike most common inbred strains of mice, BALB/c (C) is susceptible to peritoneal plasmacytomas (2) because of a complex genetic trait that includes hypomorphic (weak efficiency) alleles of genes encoding the cell cycle inhibitor $p16^{INK4a}$ (3) and the FKBP12 rapamycin-associated protein Frap (4). Peritoneal plasmacytomas do not develop spontaneously but can be readily induced by i.p. administration of proinflammatory agents such as pristane (5). Pristane provokes the formation of a chronic granulomatous tissue that provides the microenvironment in which plasmacytomas develop (6), a rich source of the plasma cell growth, differentiation, and survival factor, interleukin-6 (IL-6; ref. 7). Pristane-induced peritoneal plasmacytomas are abrogated in C mice homozygous for an *Il6* null allele (8). Plasmacytoma development also requires that the mice be maintained in a nonspecific pathogen-free (SPF) colony, which is thought to promote tumorigenesis by exposing the mice to environmental antigen (9). C mice raised in SPF or germ-free conditions exhibit a dramatically reduced plasmacytoma incidence (10) or are completely refractory to the tumors (11), respectively. Virtually all peritoneal plasmacytomas harbor a *Myc*-activating chromosomal translocation (12), which takes the form of a T(12;15)(*Igh-Myc*) in the majority (~85%) of cases. Thus, peritoneal plasmacytomas are inflammation-induced neoplasms that are dependent on the genetic background of C, IL-6, antigenic stimulation, and deregulated expression of *Myc*.

Because the development of peritoneal plasmacytomas in C mice is characterized by incomplete penetrance (tumor incidence, ≤60%) and long latency (220 days on average), efforts have been undertaken to use the enforced transgenic expression of genes known or presumed to be involved in malignant plasma cell transformation to accelerate tumor development. Efforts along this line were also aimed, in part, at inducing plasmacytomas without chronic inflammation or using SPF-maintained mice. Thus far, two approaches have been successful. The first took advantage of a widely expressed *IL6* transgene, which caused "spontaneous" plasmacytomas (no pristane) in lymphoid tissues, mostly those associated with the gut (i.e., gut-associated lymphoid tissue, GALT, plasmacytomas; ref. 13). The second approach used transgenic expression of the death repressor *BCL2* to facilitate pristane-induced peritoneal plasmacytomas in SPF-maintained mice. The *BCL2* thus eliminated the requirement for conventional husbandry of mice (14).

This study evaluated a third approach to facilitate plasmacytomagenesis in C mice: transgenic expression of *Myc*. Specifically, we sought to determine whether the $iMyc^{E\mu}$ transgene, which recreates the *Myc*-activating T(12;15) translocation that occurs in a subset (~20%) of *IL6* transgenic GALT plasmacytomas, accelerates peritoneal plasmacytomas upon introduction of C alleles to the transgenic mice. We found that the transfer of the $iMyc^{E\mu}$ transgene from a mixed genetic background of segregating *C57BL/6* (B6) × *129/SvJ* (129) alleles onto C increased the incidence of GALT plasmacytomas in first-generation backcross mice ($C.iMyc^{E\mu}$ N_1, ~75% C alleles) 2.5-fold. Tumor induction with pristane in third-generation backcross mice ($C.iMyc^{E\mu}$ N_3, ~94% C alleles) produced

Note: Supplementary data for this article are available at Cancer Research Online (http://cancerres.aacrjournals.org/).

S.S. Park, A.L. Shaffer, and J.S. Kim contributed equally to this study and should thus be considered first authors.

S.S. Park and J.S. Kim are currently at the Korea Research Institute of Bioscience and Biotechnology, Daejeon, Korea.

Requests for reprints: Siegfried Janz, Laboratory of Genetics, Center for Cancer Research, National Cancer Institute, Room 3140A, Building 37, Bethesda, MD 20892-4256. Phone: 301-496-2202; Fax: 301-402-1031; E-mail: sj4s@nih.gov.

doi:10.1158/0008-5472.CAN-05-1222

peritoneal plasmacytomas with full penetrance (100% incidence) and short latency (86 ± 28 days) compared with inbred C mice (tumor incidence, ≤60%; tumor latency, 220 ± 80 days). These results showed that C mice harboring the iMyc$^{E\mu}$ gene insertion model of the T(12;15) translocation are hypersusceptible to plasmacytoma. We conclude that the iMyc$^{E\mu}$ transgene accelerates plasmacytomas by collaborating with tumor susceptibility alleles of strain C and circumventing the requirement for tumor precursors to acquire deregulated *Myc* by somatic mutation (chromosomal translocation).

Materials and Methods

Generation of partially backcrossed C.iMyc$^{E\mu}$ mice. Strain iMyc$^{E\mu}$ was developed on the mixed genetic background of *B6* and *129* alleles using gene targeting (15). Briefly, a mouse *Myc* cDNA encoding a COOH-terminal histidine tag, His^6, was inserted into the immunoglobulin heavy-chain locus, *Igh*, just 5′ of the intronic enhancer, Eμ. To transfer the *Myc*^{His} transgene to the plasmacytoma-susceptible background of BALB/cAnPt (C), the iMyc$^{E\mu}$ mice were bred onto inbred C. Mice from the first (C.iMyc$^{E\mu}$ N_1) and third backcross generation (C.iMyc$^{E\mu}$ N_3) were used to study spontaneous tumor development and induce tumors with pristane, respectively. Mice were bred and maintained in our conventional mouse facility on the NIH campus and fed *ad libitum* Purina Mouse Chow 5001 and sterilized, acidified water. The experiments were conducted under the National Cancer Institute Animal Study Protocol LG-028.

Induction and diagnosis of peritoneal plasmacytomas. Four to 6-week-old C.iMyc$^{E\mu}$ N_3 mice were treated with two i.p. injections of 0.3-mL pristane spaced 2 months apart (days 1 and 61). Age-matched inbred C mice injected with pristane on days 1, 61, and 121 served as control. Untreated C.iMyc$^{E\mu}$ N_3 and C mice were used as additional controls. Incipient plasmacytomas were detected by monitoring the mice for the occurrence of atypical plasma cells in the peritoneal cavity. Each mouse underwent abdominal paracentesis by the insertion of a sterile 25-gauge needle and collection of a drop of peritoneal fluid. Two cytofuge slides were made and stained with May-Grünwald-Giemsa. Tumor diagnosis was established by finding ≥50 characteristic, large, hyperchromatic plasma cells on the slide. When there were <50 putative tumor cells per slide, a second confirmatory diagnosis was obtained at a later time. The diagnosis of plasmacytoma was confirmed histologically upon sacrifice of tumor-bearing mice, as described below. The tumor induction study was terminated on day 220 after pristane, >3 months after all transgenic mice had developed tumors. All surviving mice in the control groups were autopsied on day 220 to confirm that they were free of tumors.

Histology and immunohistochemistry. Four-micrometer sections of paraffin-embedded tissues were stained with H&E and in some cases with Giemsa (according to the protocol of Lennert), procedure periodic acid-Schiff, and methyl green pyronine. Nonplasmacytic lymphoid neoplasms were distinguished from plasmacytoma using criteria described in a recently proposed nomenclature for mouse hematopoietic tumors (16). Avidin-biotin immunoperoxidase techniques with antisera to IgL and IgH (Southern Biotechnology Associates, Birmingham, AL), B220 (CD45R; Caltag, Burlingame, CA), and CD19 and CD138 (syndecan-1; PharMingen, San Diego, CA) were employed for the determination of immunoglobulin production and surface marker expression.

Paraproteins. Serum paraproteins were detected with the help of Paragon SPE electrophoresis kits (Beckman Coulter, Fullerton, CA). Immunoglobulin isotypes were determined by ELISA using Immulon II plates (Dynex Technologies, Chanitlly, VA), isotype-specific goat anti-mouse serum labeled with horseradish peroxidase (Southern Biotechnology Associates), and mouse serum samples at dilutions from 10^{-3} to 1.28×10^{-5}. Plates were read on a Molecular Dynamics microplate reader at 450 nm (Sunnyvale, CA).

Allele-specific reverse transcription-PCR of *Myc* and *Myc*^{His} mRNA. For semiquantitative determination of *Myc* and *Myc*^{His} mRNA, total RNA was isolated using TRIzol (Sigma, St. Louis, MO). The integrity of RNA was verified by electrophoresis. Double-stranded cDNA was synthesized from 1 μg of total RNA, using the AMV Reverse Transcriptase kit (Roche, Indianapolis, IN). A common 5′ primer for both *Myc*^{His} and *Myc* (5′-TCTCCACTCACCAGCACAAC-3′) was combined with a specific 3′ primer for *Myc*^{His} (5′-CCTCGAGTTAGGTCAGTTTA-3′) and *Myc* (5′-ATGGT-GATGGTGATGATGAC-3′) to distinguish the two messages. Thermal cycling conditions were as follows: 95°C for 5 minutes (initial template denaturation) followed by 20 cycles of amplification at 57°C (primer annealing), 72°C (extension), and 95°C (melting), each for 1 minute. PCR amplification of *Aktb* cDNA was done for each sample as a control using the following primer pair: 5′-GCATTGTTACCAACTGGGAC-3′ (forward) and 5′-AGGCAGCTCATAGCTCTTCT-3′ (reverse). PCR products were analyzed by electrophoresis in 1% agarose gel and visualized by staining with ethidium bromide.

Microarray hybridization and analysis. Total RNA (50 μg) from each tumor, primary cell sample, or iMyc$^{E\mu}$-1 cells was labeled with cyanine 5-conjugated dUTP (Cy5). Pooled mouse cell line RNA (50 μg) was labeled with cyanine 3–conjugated dUTP (Cy3) and used as reference. Microarray hybridizations were done on Mouse Lymphochip microarrays as previously described (17). After washing, the slides were scanned using an Axon GenePix 4.0 scanner (Axon Instruments, Inc., Union City, CA). After normalization, those elements that failed to meet confidence criteria based on signal intensity and spot quality were excluded from analysis. In addition, data were discarded for any gene for which measurements were missing on >30% of the arrays or were not sequence verified. The Cy5/Cy3 intensity ratios of the remaining spots were $\log_2$ transformed. To compare the different samples, hierarchical cluster analysis was done using the Gene Cluster and Treeview programs as described previously (18). Gene expression signatures were determined statistically (t test) by comparing array elements whose expression was at least 1.8-fold different at a confidence threshold of $P < 0.0015$. The number of such element was variable dependent on the signature: 715 for the proliferation signature based on the comparison of B-cell lines and resting B cells; 146 for the B-cell signature based on the comparison of B cells and T cells; and 979 for the plasma cell signature based on the comparison of plasma cells and resting B cells. The elements identified in this way were subsequently assessed for reliability on the relevant arrays, and only elements meeting confidence criteria on 90% of the arrays were considered for analysis. Further information on microarray make-up, analysis and data interpretation is available at http://lymphochip.nih.gov/ShafferPCfactors/.

Results

Reduced survival of iMyc$^{E\mu}$ mice upon introduction of C alleles. We recently reported that ~20% of iMyc$^{E\mu}$ mice on a mixed genetic background of segregating *B6* and *129* alleles developed immunoglobulin-producing GALT plasmacytomas (15). Because plasmacytoma development in mice is a complex genetic trait, with strain C carrying several susceptibility alleles (3, 4), we hypothesized that the introduction of C alleles may accelerate GALT plasmacytomas in the iMyc$^{E\mu}$ transgenics. We thus generated C.iMyc$^{E\mu}$ N_1 mice, which contained 75% C alleles, and determined tumor onset and survival in these mice over an observation period of 530 days. Backcrossing of the iMyc$^{E\mu}$ transgene for one generation onto plasmacytoma-resistant strains 129 and C3H produced control mice that contained 75% *129* and *C3H* alleles, respectively. The introduction of C alleles resulted in the reduced survival of mice compared with the controls (Fig. 1*A*). Fourteen of 22 (63.6%) C.iMyc$^{E\mu}$ N_1 mice compared with 5 of 17 (29.4%) 129.iMyc$^{E\mu}$ N_1 mice and 3 of 24 (12.5%) C3H.iMyc$^{E\mu}$ N_1 mice were euthanized due to terminal disease or found dead by 530 days of age. The difference in survival was highly significant among the three strains using χ^2 analysis for statistical comparison of mean age at death or sacrifice ($P < 0.001$): 318 ± 79 days in the C group, 380 ± 34 days in the 129 group, and 418 ± 51 days in the C3H

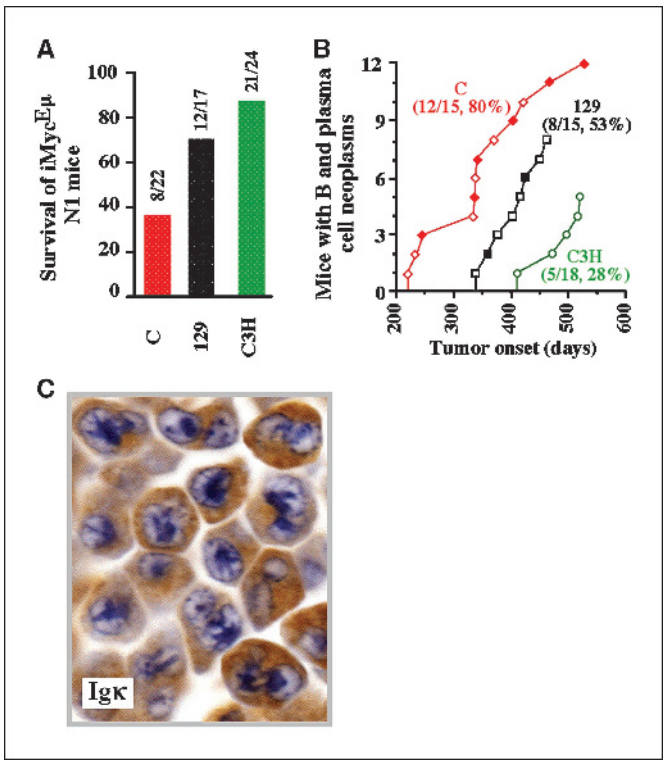

Figure 1. Reduced survival of and enhanced plasmacytoma incidence in C.iMyc^{Eμ} N_1 mice. *A,* survival of iMyc^{Eμ} mice backcrossed for one generation onto strains C, 129, or C3H followed to 530 days of age. The number of survivors and the total number of mice in each group are indicated above the columns. *B,* number and onset of plasmacytomas (*filled symbols*) and B-cell lymphomas (*open symbols*) that developed in the three strains of mice indicated in (*A*). Three, seven, and 13 mice in the C, 129, and C3H groups, respectively, did not harbor tumors. *C,* histomorphology of a typical plasmacytoma that arose in the GALT of an untreated C.iMyc^{Eμ} N_1 mice. Tumor cells contained copious amounts of cytoplasmic immunoglobulin (immunostaining for κ light chains, 63×).

group. These findings indicated that the iMyc^{Eμ} transgene causes increased mortality on the C background relative to the 129 and C3H backgrounds.

C alleles promote gut-associated lymphoid tissue plasmacytomas in iMyc^{Eμ} N_1 mice. Forty-eight mice from the above survival study were autopsied to determine the presence of neoplasia. Histologic examination of a representative panel of stained tissue sections showed that 12 of 15 (80%) C.iMyc^{Eμ} N_1 mice ranging in age from 220 to 528 days had developed B cell and plasma cell tumors (Fig. 1*B*). The tumor incidence in the 129.iMyc^{Eμ} N_1 group (8 of 15, 53%) and C3H.iMyc^{Eμ} N_1 group (5 of 18, 28%) was significantly lower than in the C.iMyc^{Eμ} N_1 group ($P < 0.01$, χ^2 analysis). Consistent with the reduced survival of C mice relative to 129 and C3H mice, the tumors occurred earlier in the C.iMyc^{Eμ} N_1 group (mean onset, 355 ± 93 days) compared with the 129.iMyc^{Eμ} N_1 (404 ± 43 days) and C3H.iMyc^{Eμ} N_1 (485 ± 46) groups ($P < 0.01$, Student's *t* test). Tumor classification according to published histologic criteria (16) revealed that 6 of 12 tumors (50%) from the C group were immunoglobulin-producing plasmacytomas (Fig. 1*B*, *filled symbols*; Fig. 1*C* presents an immunostained tissue section of one of these tumors), whereas only two of eight (25%) tumors in the 129 group and none in the C3H group had this phenotype. All other tumors were B-cell lymphomas, predominantly of the lymphoblastic B-cell lymphomas (LBL) phenotype (Fig. 1*B*, *open symbols*; ref. 15). These results suggested that the resident tumor susceptibility alleles of strain C (19, 3) accelerate the onset of *Myc*^{His}-driven neoplasia and shift the tumor pattern from B cell to plasma cell neoplasms.

C.iMyc^{Eμ} N_3 mice are hypersusceptible to peritoneal plasmacytoma. Further backcrossing of the iMyc^{Eμ} transgene onto C might lead to a strain that is highly susceptible to inflammation-induced peritoneal plasmacytomas, a type of neoplasm that develops predictably in pristane-treated C mice (5). To investigate this, we continued the backcross of *Myc*^{His} to N_3 (94% C alleles) and subjected 20 of the near congenic C.iMyc^{Eμ} N_3 mice to our standard plasmacytoma induction regimen that consists of three i.p. injections of pristane spaced 2 months apart. Tumor development was monitored by examining ascites cell specimens for the presence of neoplastic plasma cells. Strikingly, all C.iMyc^{Eμ} N_3 mice had completed tumor development before the third injection of pristane was given (114 days after the first injection of pristane; Fig. 2*A*, *filled squares*). Mean tumor latency was 86 ± 28 days. Tumor classification (16) showed that with the exception of one tumor that was a B-cell lymphoma, 19 of 20 (95%) neoplasms were plasmacytomas (Fig. 2*B*). Among 40 pristane-treated C mice included as control, only two mice (5%) had developed plasmacytoma by day 150 after pristane (Fig. 2*A*, *filled diamonds*). Consistent with previous observations that non-SPF maintained C mice require three injections of pristane to develop 40% to 60% peritoneal plasmacytomas by day 300 (20), the third injection of pristane on day 120 resulted in an increase in tumor incidence to 25% by day 175. Untreated C mice ($n = 26$) remained tumor free throughout the observation period (Fig. 2*A*, *open diamond*). In line with the tumor onset in untreated C.iMyc^{Eμ} N_1 mice (Fig. 1), 4 of 47 (8.5%) untreated C.iMyc^{Eμ} N_3 mice developed neoplasms spontaneously (no pristane): two lymphomas (LBL) and two plasma cell tumors (Fig. 2*A*, *open squares*). These findings showed that the *Myc*^{His} *Myc*^{His} transgene on the C background cooperates with tissue factors in the pristane granuloma, most likely including IL-6 (7, 21), to greatly facilitate peritoneal plasmacytomas.

Features of plasmacytoma. Histologic examination of peritoneal plasmacytomas from C.iMyc^{Eμ} N_3 mice revealed three tumor subtypes: plasmacytic tumors, the predominant type in inbred C mice (22); less mature, plasmablastic tumors, the most common type in the present sample (Fig. 2*B*); and anaplastic tumors, which were characterized by the admixture of pleomorphic plasma cells with aberrant immunoblasts and plasmablasts (Supplementary Fig. S1). Regardless of histologic subtype, plasmacytomas expressed high levels of *Myc*^{His} mRNA (Fig. 2*C*) and, as expected, very low or undetectable levels of normal *Myc* mRNA (data not shown), using reverse transcription-PCR analysis. One tumor (*lane 6*) was exceptional because it expressed *Myc* instead of *Myc*^{His} for reasons that remained unknown. Fractionation of serum proteins by electrophoresis readily showed M components in mice harboring primary (G_0) and transplanted (G_1-G_2) tumors (Fig. 2*D*). The M spikes were usually less pronounced in G_0 mice, particularly those with anaplastic plasmacytoma (data not shown). Immunohistochemical analysis using antibodies to immunoglobulin heavy chains showed considerable clonal diversity among the malignant plasma cells at G_0, with abundant α expressing cell clones coexisting with μ and γ expressing cell clones in the same mouse (data not shown). Immunostaining of nine transplanted plasmacytomas together with ELISA-based isotyping of serum immunoglobulin spikes in tumor-bearing G_1-G_2 mice showed that seven of these tumors produced α heavy chains (data not shown). This established an important parallel to transplanted plasmacytomas

in inbred C mice, in which IgA is also the preferred isotype (~60%; ref. 1). Transfer of cell suspensions from plasmacytoma-infiltrated granulomatous tissues on days 76 and 81 after pristane into the peritoneal cavity of pristane-primed C mice resulted in the outgrowth of tumors in two of two and six of eight cases, respectively. Tumor cells were also propagated by s.c. injection (data not shown). This indicated that the presumptive tumor cells were indeed fully transformed.

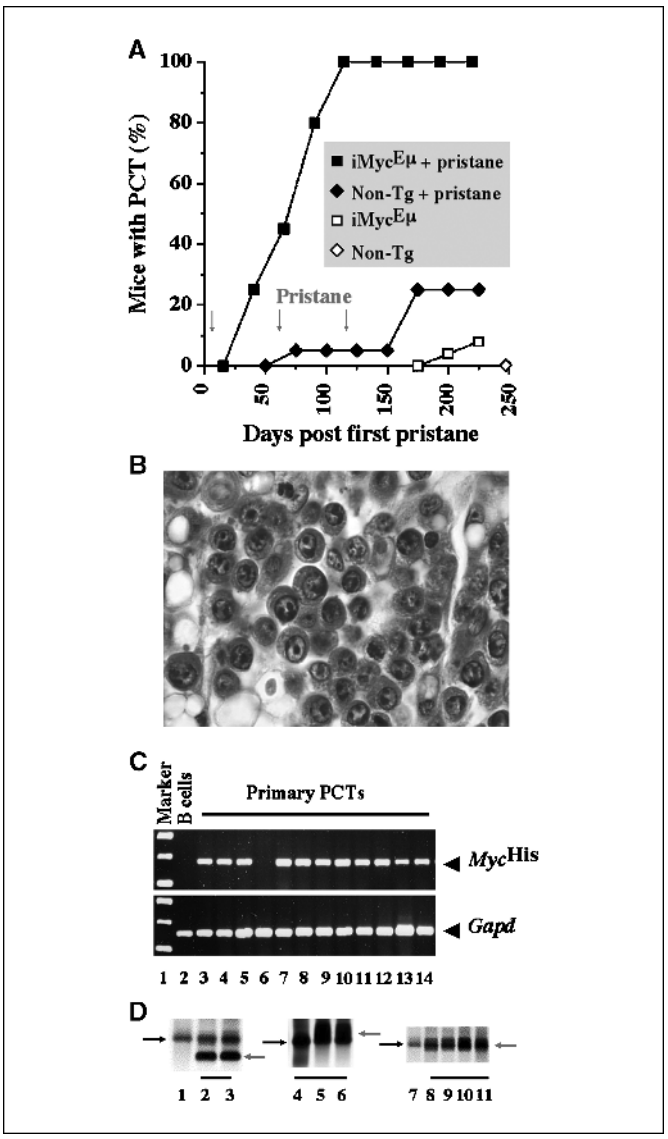

Figure 2. Accelerated peritoneal plasmacytomas (*PCT*) in C.iMyc$^{E\mu}$ N_3 mice. *A,* onset and incidence of plasmacytomas in pristane-treated and untreated C.iMyc$^{E\mu}$ N_3 mice and their nontransgenic littermates. All mice received three injections of 0.3-mL pristane on days 1, 60, and 120 (*red arrows pointing down*), except the C.iMyc$^{E\mu}$ N_3 group, which did not receive the third injection. *B,* histomorphology of a typical peritoneal plasmacytoma that developed in a pristane-treated C.iMyc$^{E\mu}$ N_3 mouse. *C,* reverse transcription-PCR analysis of *Myc*^{His} mRNA (*top*) and *Gapd* mRNA (*bottom*) in plasmacytomas and normal B cells (*lane 2*). *Lane 1,* size marker. *D,* monoclonal immunoglobulins in sera and ascites of plasmacytoma-harboring mice. Protein electropherograms of untreated C mice (*control*; *lanes 1* and *7*) and C.iMyc$^{E\mu}$ N_3 mice containing primary plasmacytomas (*lanes 4* and *8*) or transplanted plasmacytomas propagated once (G_1 tumors; *lanes 2*, *3*, *5*, *6*, *9*, and *10*) or twice (G_2 tumor; *lane 11*). *Lanes 2*, *5*, *9*, *11,* serum samples; *lanes 3*, *6*, and *10,* ascites samples. Black horizontal lines designate related samples. Normal γ-globulins (*black arrows*) and M spikes (*red arrows*).

Gene expression profile of iMyc$^{E\mu}$ plasmacytomas. The mouse Lymphochip, a microarray of hematopoietic mouse cDNA clones, provides a powerful tool to classify mouse B cell and plasma cell tumors based on global gene expression programs (23). To determine the gene expression profile of the pristane-induced peritoneal plasmacytomas that arose in the iMyc$^{E\mu}$ N_3 mice, RNA samples from the abovementioned nine G_1 tumors were analyzed. LBL from iMyc$^{E\mu}$ mice (15), pristane-induced plasmacytomas from inbred C mice, resting and activated mouse B and T cells, and mouse embryonic fibroblasts (MEF) were included for comparison. A total of 4,500 array elements that fulfilled all statistical confidence criteria and were present on at least 90% of all arrays were clustered across the samples based on gene expression patterns. Nearly a quarter of these elements (1,010, 22.4%) showed a 1.8-fold minimal difference in average expression in plasmacytomas and LBLs ($P < 0.015$, t test). Cluster analysis (presented in Supplementary Fig. 2) showed a striking distinction between the two neoplastic cell types, plasmacytoma and LBL. Indeed, the comparison of individual plasmacytoma and LBL expression profiles with each other revealed a remarkable homogeneity among the iMyc$^{E\mu}$ tumors, which clustered in two tight groups. Among the normal samples, lymphoid and non-lymphoid cell types (B/T cells versus MEF), lymphocyte lineages (B versus T cells), and lymphocyte activation states [resting B and T cells versus *in vitro* stimulated cells using lipopolysaccharide (LPS) and antibody to CD3, respectively] were also clearly separated by hierarchical clustering (Supplementary Fig. S2). These results provided evidence at the transcriptional level that peritoneal plasmacytomas in C.iMyc$^{E\mu}$ N_3 mice constitute a unique type of neoplasm, clearly different from LBL, the predominant tumor in untreated iMyc$^{E\mu}$ mice on the mixed *B6* × *129* background (15).

Gene expression signatures of iMyc$^{E\mu}$ plasmacytomas. To further examine the differences in the gene expression profile of the iMyc$^{E\mu}$ plasmacytoma and LBL samples, genes from three distinct "signature" clusters (24), designated plasma cell signature, B-cell signature, and proliferation signature, were analyzed. The signatures are presented in Fig. 3, each annotated with ten differentially expressed genes in plasmacytoma compared with LBL. The expression levels of these genes are shown in Table 1.

Consistent with their differentiation status, the plasmacytomas overexpressed many genes in the plasma cell signature compared with the LBLs. The average expression of genes in this signature was significantly higher in the plasmacytomas than in the LBLs (data not shown). A majority of genes in the signature (93%) was overexpressed in the plasmacytoma compared with the LBL sample (Supplementary Table S1). The most highly up-regulated genes in plasmacytoma included the immunoglobulin joining gene *Igj* and genes involved in protein synthesis and secretion (*Ell2*, *Edem1*, and *Sec61a*) and cytokine signaling (*Socs2*). Similar to human plasma cells (25), genes involved in antioxidative defense (e.g., *Prdx4*, *Aldh1*, and *Grx1*) were conspicuously present in the mouse plasma cell tumors (Supplementary Table 1). In addition, *Xbp1*, a key player in the terminal differentiation of B lymphocytes to plasma cells (26, 18), was highly expressed in plasmacytomas compared with LBLs.

Plasmacytomas underexpressed the majority of genes in the B-cell signature upon comparison to LBLs (17 of 30, 57%, Supplementary Table 2). Examples include genes that encode the μ-heavy chain (*Igh6*), various B-cell differentiation markers (*Cd79a*, *Cd79b*, and *Cd19*), and the Fcγ2b receptor (*Fcgr2b*; Fig. 3).

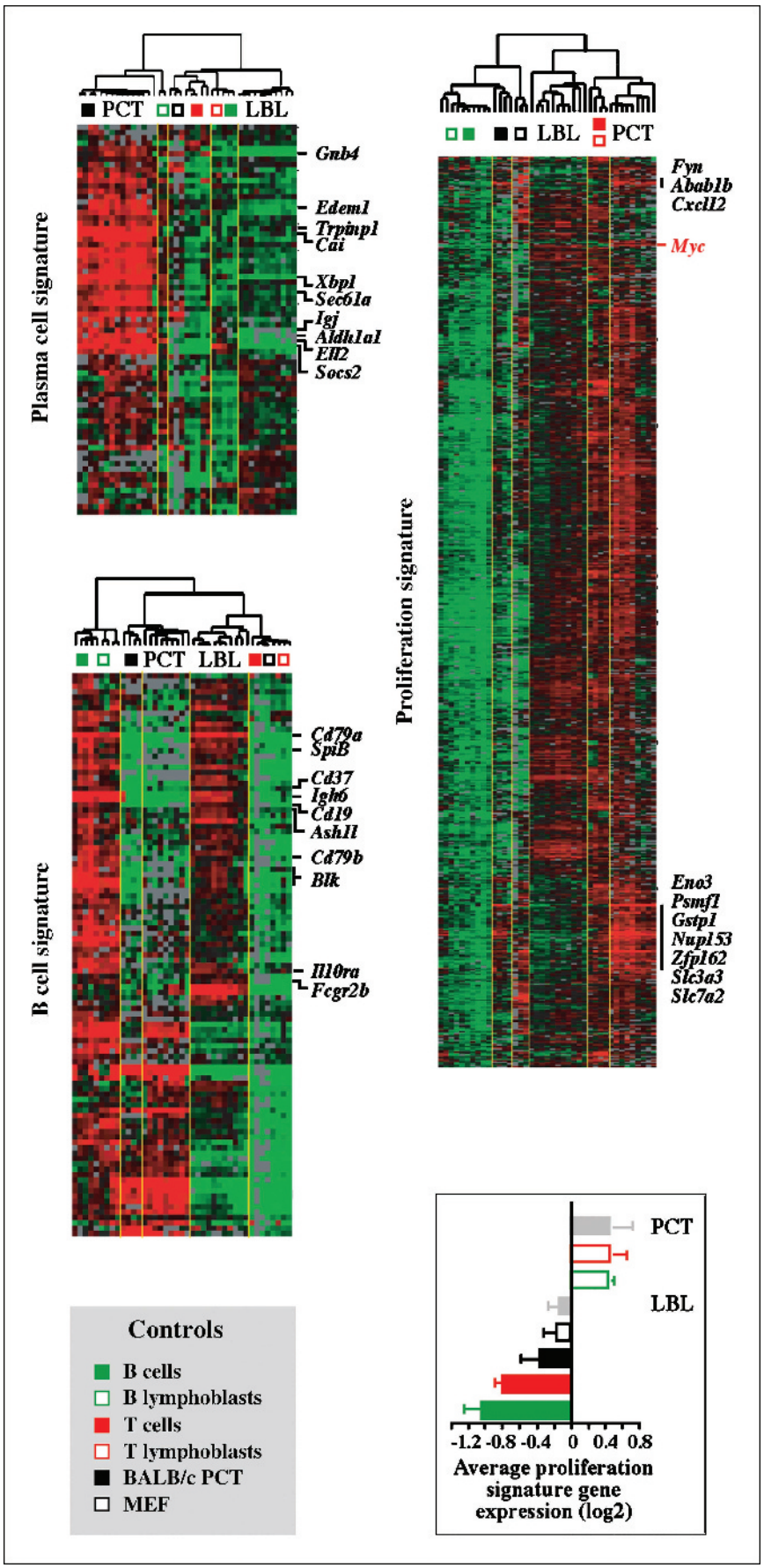

Figure 3. Gene expression profiles of peritoneal plasmacytoma (*PCT*) on mouse Lymphochip cDNA microarrays. Compared to LBLs, plasmacytomas were characterized by the high expression of plasma cell and proliferation signature genes including *Myc* (*red*) but low expression of B-cell signature genes. The location of selected genes in the three different signature clusters is indicated by official gene symbols (see Table 1 for additional information). Control samples are indicated in the gray text box by open or filled squares that are labeled. B lymphoblasts were MACS-purified $B220^{+}$ splenocytes stimulated with LPS for 48 hours. T lymphoblasts were activated by antibody to CD3 for 24 hours. The average expression of genes in the proliferation signature is plotted below this signature for plasmacytomas and LBLs (*gray columns*) and the six control samples shown in the text box. SDs are indicated by horizontal lines.

Table 1. Ten most differentially regulated plasma cell, B cell, and proliferation signature genes in PCT and LBL from iMyc$^{E\mu}$ mice

Gene symbol	Gene signature and name	Relative gene expression					*P* (*t* test) (PCT versus LBL)
		PCT		LBL		PCT/LBL (real fold)	
		Mean (log_2)	SD	Mean (log2)	SD		
Plasma cell signature							
Aldh1a1	Aldehyde dehydrogenase family 1, subfamily A1	2.03	0.555	−1.87	0.666	14.9	4.24×10^{-8}
Cai	Calcium-binding protein, intestinal	3.13	0.708	−0.621	0.586	13.5	1.54×10^{-10}
Gnb4	Guanine nucleotide binding protein, β 4	1.16	0.510	−4.06	0.837	37.2	$3.69 \times 4\ 10^{-12}$
Ell2	Elongation factor RNA polymerase II 2	2.16	0.715	−1.58	0.405	13.3	$7.40 \times 4\ 10^{-10}$
Edem1	ER degradation enhancer, mannosidase α-like 1	1.77	0.460	−1.11	0.269	7.3	6.14×10^{-11}
Igj	Immunoglobulin joining chain	1.21	0.823	−2.71	1.32	15.1	1.03×10^{-3}
Sec61a	Sec61 α 1 subunit (*Saccharomyces cerevisiae*)	2.51	0.486	−0.334	0.312	7.2	8.80×10^{-11}
Socs2	Suppressor of cytokine signaling 2	2.63	0.656	−2.21	0.261	28.6	9.46×10^{-11}
Trp53inp1	Transformation-related protein 53 inducible nuclear protein 1	2.80	0.766	−0.503	0.385	9.8	1.59×10^{-8}
Xbp1	X-box binding protein 1	3.93	0.780	−1.32	0.315	38.2	2.44×10^{-10}
B-cell signature							
Ash1l	Ash1 (absent, small, or homeotic)-like	−0.633	0.492	0.446	0.677	0.474	4.99×10^{-6}
Blk	B lymphoid kinase	−0.858	0.739	0.031	0.709	0.540	3.37×10^{-3}
Cd19	CD19 antigen	−7.06	2.77	0.354	4.01	0.00589	1.80×10^{-7}
Cd37	CD37 antigen	−1.45	0.652	0.825	1.22	0.00589	1.92×10^{-8}
Cd79a	CD79a antigen (Iga)	−6.49	0.757	2.13	4.67	0.00255	9.74×10^{-9}
Cd79b	CD79b antigen (Igβ)	−1.28	0.757	1.73	0.467	0.276	5.26×10^{-6}
Fcgr2b	Fc receptor, IgG, low affinity IIb	−0.797	0.622	0.438	0.769	0.425	2.94×10^{-5}
Igh6	Immunoglobulin μ heavy chain	−4.40	3.11	1.14	3.47	0.0215	1.91×10^{-5}
Il10ra	IL-10 receptor α	−0.448	3.20	0.590	0.714	0.487	1.62×10^{-3}
Spi-B	Spi-B transcription factor (PU.1 related)	−0.633	0.492	0.446	0.677	0.473	1.37×10^{-3}
Proliferation signature							
Abcb1b	ATP-binding cassette, subfamily B, member 1B	0.795	0.656	−1.62	0.693	5.33	5.10×10^{-6}
Cxcl12	Chemokine ligand 12	2.03	0.843	0.115	0.722	3.77	1.50×10^{-4}
Eno3	Enolase 3, β muscle	2.39	0.574	−0.451	0.513	7.17	7.68×10^{-10}
Fyn	Fyn proto-oncogene	1.23	0.619	−0.538	0.354	3.17	1.28×10^{-6}
Gstp1	Glutathione *S*-transferase, pi 1	1.15	0.487	−0.638	0.354	3.44	1.99×10^{-8}
Nup153	Nucleoporin 153	2.76	0.498	−0.775	0.307	11.6	1.48×10^{-13}
Psmf1	Proteasome inhibitor subunit 1	2.41	0.542	−0.303	0.753	6.55	4.16×10^{-8}
Slc3a2	Solute carrier family 3, member 2	1.72	0.304	−0.642	0.323	5.14	2.18×10^{-12}
Slc7a5	Solute carrier family 7, member 5	2.15	0.513	−0.378	0.343	5.77	1.10×10^{-10}
Zfp162	Zinc finger protein 162	1.98	0.751	−0.132	0.499	4.32	5.73×10^{-7}

Abbreviation: PCT, plasmacytoma.

Plasmacytomas showed very high expression levels of proliferation signature genes (Fig. 3). The graph below the proliferation signature cluster in Fig. 3 shows that the average expression of genes in this signature was identical to that seen in T and B lymphocytes acutely activated with antibody to CD3 (for 24 hours) and LPS (for 48 hours), respectively. The average expression of proliferation signature genes in plasmacytomas was significantly higher than in LBLs, pristane-induced plasma cell tumors from inbred C mice (*filled black column*), and controls (MEF, *black open column*; resting B and T cells, *filled green* and *red columns*, respectively). This finding agreed with the overall *Myc* level of *Myc*^{His}-induced tumors, which was ~2-fold higher in the plasmacytomas than the LBLs. The *Myc* levels correlated, in turn, with the average expression of known Myc target genes (http://www.myc-cancer-gene.org), which was 1.96-fold elevated in the plasmacytoma compared with the LBL sample (data not shown). Of a total of 246 genes in the proliferation signature, 204 (83%) genes were overexpressed in the plasmacytomas relative to the LBLs (data not shown). Seventeen of the 204 (8%) genes, among them four known Myc targets (*Nup153*, *Slc7a5*, *Hars*, and *Gstp1*), were >3-fold elevated in the plasmacytomas (Supplementary Table S3).

These results showed that plasmacytomas are *Myc*^{His}-induced neoplasms that exhibit a unique gene expression pattern globally (Supplementary Fig. S2) at the level of three different gene expression signatures (Fig. 3), and for numerous individual genes, such as *Myc* and *Xbp1*.

Abundant plasmacytoma precursor lesions in pristane-treated C.iMyc$^{E\mu}$ N$_3$ mice. Peritoneal plasmacytomas in inbred C mice are preceded by the premalignant precursor lesion, plasmacytic focus, which is defined as a dense aggregate of ≥50 hyperchromatic plasma cells in a microscopic field of ~1 mm^2. Abundance and size of foci are correlated with the genetic

susceptibility to peritoneal plasmacytoma. Foci are routinely encountered in plasmacytoma-susceptible C mice 75 to 100 days after pristane but are rarely seen earlier (22). To determine whether accelerated plasmacytomagenesis in C.iMyc$^{E\mu}$ N_3 mice was associated with the accelerated development of plasmacytic foci, mesenteric pristane granulomas were obtained on days 14 and 37 after injection of 0.3-mL pristane. Foci were large and highly abundant (Fig. 4*A*) and frequently associated with increased numbers of blood vessels, possibly reflecting *Myc*^{His}-induced angiogenesis (ref. 27; Fig. 4*B*). Immunostaining showed that foci produced a variety of immunoglobulin isotypes, prominently including IgA (Fig. 4*C* and *D*). Antibody to phosphohistone H3 (marker of mitosis) revealed high levels of proliferation (Fig. 4*E* and *F*), a stark contrast to the very low levels of cell division determined by microscopic enumeration of mitotic figures in foci of C mice (mean mitotic index, 0.74%; ref. 22). Consistent with the elevated proliferation levels of foci in C.iMyc$^{E\mu}$ mice compared with C mice, the cellular composition of foci was different in the two mouse strains. Whereas mature plasma cells predominate in C mice, plasmablasts, immunoblast-like cells, and aberrant plasma cells were highly abundant in C.iMyc$^{E\mu}$ mice. These results established that plasmacytomagenesis in C.iMyc$^{E\mu}$ mice is accompanied by the accelerated development of hyperproliferative tumor precursor lesions.

Premalignant plasmablasts undergo isotype switching *in situ*. To determine whether cells from plasmacytic foci were transplantable, single-cell suspensions were prepared from peritoneal granulomas of C.iMyc$^{E\mu}$ N_3 mice on day 14 (eight mice) and day 26 (nine mice) after pristane. The transfer of these cells to C mice primed by i.p. inoculation with pristane was unsuccessful in all cases, showing that the plasmablasts and plasma cells at this early stage of tumor development are not yet fully transformed. To analyze the differentiation status of the cells in the foci, double staining of tissue sections with antibody to B220 (B cell marker) and cytoplasmic Igκ (plasma cell marker) was done. Foci in C.iMyc$^{E\mu}$ N_3 mice were often composed of a core of B cells surrounded by a mantle of plasmablasts and plasma cells (Supplementary Fig. S3), suggesting that the B cell to plasma cell transition occurs *in situ*. Staining of serial sections with antibody to μ and α heavy chains and Ki67 showed that IgM$^+$ cells intermingled with IgA$^+$ cells and that both cell types were actively cycling (Supplementary Fig. S4). This suggested that isotype switching takes place in clonally related plasmablasts *in situ*. The repeated codetection of $\mu^+\lambda^+$ and $\alpha^+\lambda^+$ plasmablasts in the same focus lent support to this interpretation. Because λ expression is rare in mice (~5% of B cells), it is highly improbable (~1:400) that $\mu^+\lambda^{+?}$ and $\alpha^+\lambda^+$ plasmablasts that are not clonally related to each other coexist in the narrow space of the same focus, like the one shown in Supplementary Fig. S5. The presence

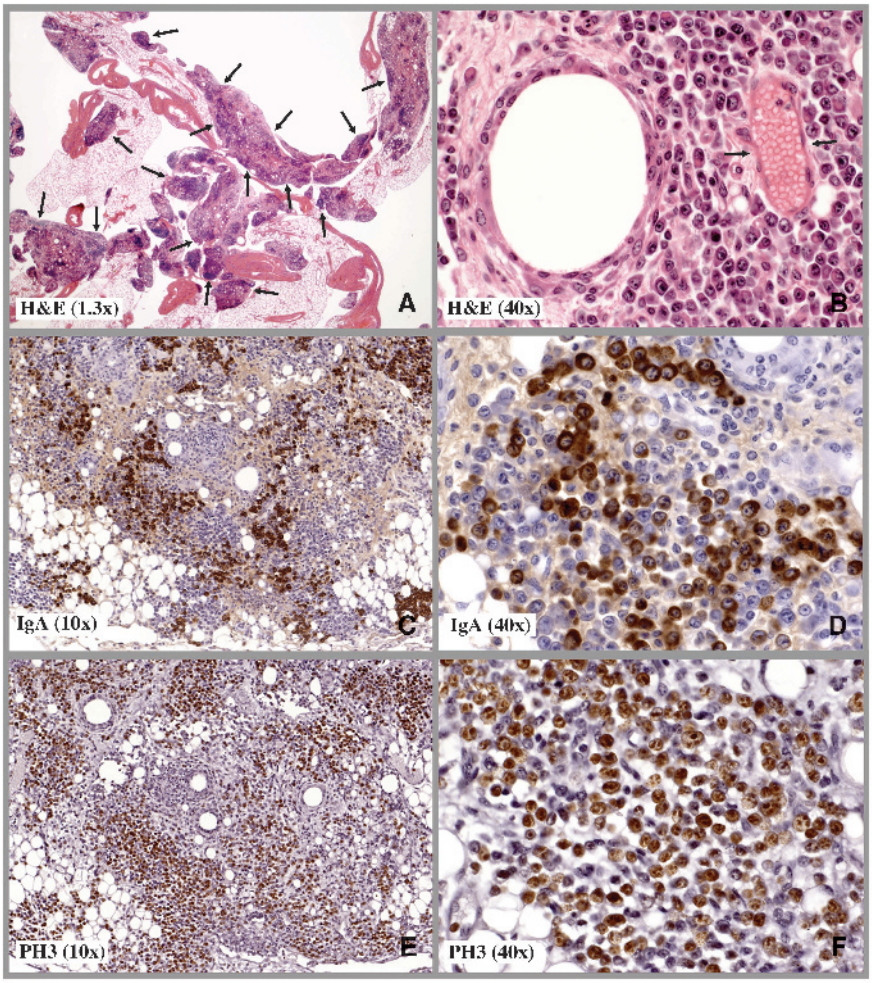

Figure 4. Plasmacytoma precursor lesions in pristane-treated C.iMyc$^{E\mu}$ N_3 mice. Low-power microscopy (*A*) shows that inflammatory granulomas of C.iMyc$^{E\mu}$ N_3 mice harbor abundant plasmablastic/plasmacytic foci (*arrows*) as early as 14 days after pristane. Higher magnification demonstrated that foci are often associated with small blood vessels (*arrows* in *B*) and contain large numbers of IgA-producing cells (*C* and *D*) that are actively cycling, as shown by immunostaining with antibody to phosphohistone H3 (*E* and *F*).

of T cells many B-cell aggregates, including the one depicted in Supplementary Fig. 3, was also consistent with isotype switching *in situ* (Supplementary Fig. S6).

Discussion

The main finding of this study is the acceleration of plasmacytoma development in partially backcrossed C.iMyc$^{E\mu}$ mice. Unlike strain C, in which peritoneal plasmacytomas take on average 220 days to develop and tumor incidence rarely exceeds 60% by day 300 after tumor induction with three injections of pristane, peritoneal plasmacytomas in C.iMyc$^{E\mu}$ N_3 mice developed with a mean tumor onset of 86 days and full penetrance (100% incidence) after two injections of pristane. This observation extended previous findings on the collaboration of deregulated *Myc* with tumor susceptibility alleles of strain C in plasmacytoma development (13, 14). Furthermore, it strengthened our contention that absent the ability to predictably induce T(12;15) translocations in mouse B cells and plasma cells (28), the insertion of *Myc* into the *Igh* locus of gene-targeted mice provides a good solution to mimicking this translocation in a manner conducive to plasmacytoma development (15).

The C.iMyc$^{E\mu}$ model of accelerated plasmacytomagenesis extends two previous approaches to facilitate plasmacytomas by enforced expression of *Myc*: infection of mice with *Myc*-encoding retrovirus and transgenic expression of *Myc* under control of immunoglobulin enhancers. Although these approaches successfully bypassed the requirement of incipient tumor cells to acquire "active" *Myc* by chromosomal translocation, they exhibited serious shortcomings compared with the present gene insertion model of T(12;15) translocation. RIM virus (coexpression of c-*Myc* and v-Ha-*Ras*; ref. 29) and J3V1 virus (v-*Myc* and v-*Raf*; refs. 30, 31) induced mainly IgM$^+$ tumors, indicating that the virus transformed pre-germinal center B cells before isotype switching. ABL/MYC virus (v-*Abl* and c-*Myc*; ref. 32) was able to overcome this limitation by inducing "post-switch" neoplasms; however, these tumors exhibited the unusual feature of developing without CD4$^+$ T-cell help (33), an essential cofactor for normal isotype switching (34) and peritoneal plasmacytomagenesis in C mice (35). Among the various mouse strains carrying *Myc* transgenes driven by immunoglobulin enhancers (36–41), none has been reported thus far to induce plasma cell neoplasms as the predominant tumor type. Supplementation of *Myc* with a second transgene resulted in one case in a striking shift in the tumor spectrum from B-cell lymphomas in the "*Myc* only" mice to plasma cell tumors in the double transgenic mice: Eμ-Myc and v-Abl (42). Although this finding suggests that introduction of *Abl* to strain C.iMyc$^{E\mu}$ leads to further acceleration of plasmacytoma, it remains unclear whether this manipulation would recapitulate the natural history of tumor development. One point of caution is that *Abl* was similarly expressed on the mouse lymphochips in plasmacytoma and LBL from C.iMyc$^{E\mu}$ mice (data not shown).

The demonstration that C.iMyc$^{E\mu}$ mice are hypersusceptible to plasmacytoma generates an apparent conundrum with respect to previous reports on the abundance of T(12;15)-harboring cell clones in tumor-free C mice (reviewed in ref. 43). The repeated detection by PCR of reciprocal *Igh-Myc* junction fragments, the molecular indicators of T(12;15), indicated that translocation-carrying cells are generated in great numbers at early stages of tumor development (44). This resulted in the hypothesis that the T(12;15) translocation, a tumor-initiating event, is not rate limiting for plasmacytomagenesis (43). The present study raises the question why the recapitulation of a pathogenetic event that may not slow down tumor development in the first place (i.e., *Myc* translocation) would facilitate plasmacytoma. The apparent contradiction may be reconciled if one considers that genomic PCR amplification of *Igh-Myc* junctions shows the presence of translocation-carrying cells but does not inform whether these cells contain up- or de-regulated *Myc*. If a large number of T(12;15)$^+$ cells were excluded from the tumor precursor pool due to inappropriate or fluctuating *Myc* levels, *Myc* translocation might still be rate limiting despite the abundant detection of translocation-bearing cells by PCR. Cells with acute spikes in *Myc* expression may be eliminated *in vivo* by *Myc*-dependent apoptosis (45), whereas cells with insufficient *Myc* levels may linger in a state of hypoproliferation reminiscent of the kind of tumor dormancy seen upon down-regulation of *Myc* in certain neoplasms (46). Further studies are warranted to determine the variability of *Myc* expression in T(12;15)-harboring plasmacytoma precursors (47) and define the (presumably narrow) range of *Myc* expression that is permissive for plasmacytoma development (48).

This study shows, for the first time, the utility of the mouse Lymphochip cDNA gene array for comparisons of gene expression profiles of primary and transplanted B cell and plasma cell tumors in mice. Array analysis clearly showed that plasmacytomas had retained the expression of the plasma cell signature but down regulated the B cell gene expression program. Apparently, the inserted "iMyc" did neither interrupt the differentiation potential of tumor precursors to mature into plasma cells nor interfere with the ability of these cells to retain the plasma cell phenotype upon transplantation. These findings suggest that the targeting of genes essential for plasma cells might lead to new interventions to plasma cell tumors in humans. Abrogation of *XBP1*, a crucial gene in normal plasma cells (49) that is also highly expressed in the present mouse plasmacytomas, has recently been proposed as a means to improve the clinical outcome of human multiple myeloma (50). Gene array analysis may further reveal new targets of tumor therapy by comparing the gene expression program in normal and neoplastic plasma cells. One obvious example may be *Myc*. Similar to advanced multiple myeloma, mouse plasmacytomas overexpress *Myc*, whereas normal plasma cells down-regulate *Myc* concomitant with cessation of cell cycling (51, 26). Targeting the mechanism that overrides suppression of *Myc* in neoplastic plasma cell may be of great therapeutic value.

In conclusion, this study presents a genetically defined and manipulable mouse model of inflammation-dependent plasma cell neoplasia that takes advantage of the iMyc$^{E\mu}$ transgene and tumor susceptibility alleles of strain C to greatly accelerate tumor development. The robustness of the present plasmacytoma model (short onset, complete penetrance) may facilitate ongoing studies on the natural history of plasma cell neoplasms and inform the design of new approaches to prevent and treat these neoplasms in human beings.

Acknowledgments

Received 4/7/2005; revised 6/18/2005; accepted 6/28/2005.

The costs of publication of this article were defrayed in part by the payment of page charges. This article must therefore be hereby marked *advertisement* in accordance with 18 U.S.C. Section 1734 solely to indicate this fact.

We thank Nicole Wrice, Tina Wellington, and Vaishali Jarrar (National Cancer Institute, NCI) for assistance with the *in vivo* studies; Seung Tae Chung (NCI) for genotyping; Seung-Su Han (NCI) for determining *Myc*^{His} expression using PCR; Elizabeth B. Mushinski (NCI) for immunostaining; and Beverly A. Mock (NCI) for support.

References

1. Potter M. Neoplastic development in plasma cells. Immunol Rev 2003;194:177–95.
2. Potter M, Pumphrey JG, Bailey DW. Genetics of susceptibility to plasmacytoma induction. I. BALB/cAnN (C), C57BL/6N (B6), C57BL/Ka (BK), (C times B6)F1, (C times BK)F1, and C times B recombinant-inbred strains. J Natl Cancer Inst 1975;54:1413–7.
3. Zhang SL, DuBois W, Ramsay ES, et al. Efficiency alleles of the pctr1 modifier locus for plasmacytoma susceptibility. Mol Cell Biol 2001;21:310–8.
4. Bliskovsky V, Ramsay ES, Scott J, et al. Frap, FKBP12 rapamycin-associated protein, is a candidate gene for the plasmacytoma resistance locus Pctr2 and can act as a tumor suppressor gene. Proc Natl Acad Sci U S A 2003; 100:14982–7.
5. Anderson PN, Potter M. Induction of plasma cell tumours in BALB-c mice with 2,6,10,14-tetramethylpentadecane (pristane). Nature 1969;222:994–5.
6. Potter M, MacCardle RC. Histology of developing plasma cell neoplasia induced by mineral oil in BALB/c mice. J Natl Cancer Inst 1964;33:497.
7. Shacter E, Arzadon GK, Williams J. Elevation of interleukin-6 in response to a chronic inflammatory stimulus in mice: inhibition by indomethacin. Blood 1992; 80:194–202.
8. Lattanzio G, Libert C, Aquilina M, et al. Defective development of pristane-oil-induced plasmacytomas in interleukin-6-deficient BALB/c mice. Am J Pathol 1997; 151:689–96.
9. Niiro H, Clark EA. Regulation of B-cell fate by antigen-receptor signals. Nat Rev Immunol 2002;2:945–56.
10. Byrd LG, McDonald AH, Gold LG, Potter M. Specific pathogen-free BALB/cAn mice are refractory to plasmacytoma induction by pristane. J Immunol 1991;147: 3632–7.
11. McIntire KR, Princler GL. Prolonged adjuvant stimulation in germ-free BALB-c mice: development of plasma cell neoplasia. Immunology 1969;17:481–7.
12. Shen-Ong GL, Keath EJ, Piccoli SP, Cole MD. Novel myc oncogene RNA from abortive immunoglobulin-gene recombination in mouse plasmacytomas. Cell 1982; 31:443–52.
13. Kovalchuk AL, Kim JS, Park SS, et al. IL-6 transgenic mouse model for extraosseous plasmacytoma. Proc Natl Acad Sci U S A 2002;99:1509–14.
14. Silva S, Kovalchuk AL, Kim JS, Klein G, Janz S. BCL2 accelerates inflammation-induced BALB/c plasmacytomas and promotes novel tumors with coexisting T(12;15) and T(6;15) translocations. Cancer Res 2003; 63:8656–63.
15. Park SS, Kim JS, Tessarollo L, et al. Insertion of c-Myc into Igh induces B-cell and plasma-cell neoplasms in mice. Cancer Res 2005;65:1306–15.
16. Morse HC III, Anver MR, Fredrickson TN, et al. Bethesda proposals for classification of lymphoid neoplasms in mice. Blood 2002;100:246–58.
17. Shaffer AL, Yu X, He Y, et al. BCL-6 represses genes that function in lymphocyte differentiation, inflammation, and cell cycle control. Immunity 2000;13:199–212.
18. Shaffer AL, Shapiro-Shelef M, Iwakoshi NN, et al. XBP1, downstream of Blimp-1, expands the secretory apparatus and other organelles, and increases protein synthesis in plasma cell differentiation. Immunity 2004; 21:81–93.
19. Zhang S, Ramsay ES, Mock BA. Cdkn2a, the cyclin-dependent kinase inhibitor encoding p16INK4a and p19ARF, is a candidate for the plasmacytoma susceptibility locus, Pctr1. Proc Natl Acad Sci U S A 1998;95: 2429–34.
20. Potter M, Wax JS. Peritoneal plasmacytomagenesis in mice: comparison of different pristane dose regimens. J Natl Cancer Inst 1983;71:391–5.
21. Hinson RM, Williams JA, Shacter E. Elevated interleukin 6 is induced by prostaglandin E2 in a murine model of inflammation: possible role of cyclooxygenase-2. Proc Natl Acad Sci U S A 1996;93: 4885–90.
22. Potter M, Mushinski EB, Wax JS, Hartley J, Mock BA. Identification of two genes on chromosome 4 that determine resistance to plasmacytoma induction in mice. Cancer Res 1994;54:969–75.
23. Alizadeh A, Eisen M, Davis RE, et al. The lymphochip: a specialized cDNA microarray for the genomic-scale analysis of gene expression in normal and malignant lymphocytes. Cold Spring Harb Symp Quant Biol 1999; 64:71–8.
24. Shaffer AL, Rosenwald A, Hurt EM, et al. Signatures of the immune response. Immunity 2001;15:375–85.
25. Tarte K, Zhan F, De Vos J, Klein B, Shaughnessy J Jr. Gene expression profiling of plasma cells and plasmablasts: toward a better understanding of the late stages of B-cell differentiation. Blood 2003;102:592–600.
26. Shaffer AL, Lin KI, Kuo TC, et al. Blimp-1 orchestrates plasma cell differentiation by extinguishing the mature B cell gene expression program. Immunity 2002; 17:51–62.
27. Baudino TA, McKay C, Pendeville-Samain H, et al. c-Myc is essential for vasculogenesis and angiogenesis during development and tumor progression. Genes Dev 2002;16:2530–43.
28. Smith AJ, De Sousa MA, Kwabi-Addo B, et al. A site-directed chromosomal translocation induced in embryonic stem cells by Cre-loxP recombination. Nat Genet 1995;9:376–85.
29. Clynes R, Wax J, Stanton LW, et al. Rapid induction of IgM-secreting murine plasmacytomas by pristane and an immunoglobulin heavy-chain promoter/enhancer-driven c-*myc*/v-Ha-ras retrovirus. Proc Natl Acad Sci U S A 1988;85:6067–71.
30. Potter M, Mushinski JF, Mushinski EB, et al. Avian v-myc replaces chromosomal translocation in murine plasmacytomagenesis. Science 1987;235:787–9.
31. Troppmair J, Potter M, Wax JS, Rapp UR. An altered v-raf is required in addition to v-myc in J3V1 virus for acceleration of murine plasmacytomagenesis. Proc Natl Acad Sci U S A 1989;86:9941–5.
32. Largaespada DA, Kaehler DA, Mishak H, et al. A retrovirus that expresses v-abl and c-*myc* oncogenes rapidly induces plasmacytomas. Oncogene 1992;7:811–9.
33. Weissinger EM, Byrd LG, Henderson DW, Mushinski JF. Overexpression of v-abl uniquely cooperates with c-*myc* dysregulation in induction of plasma cell tumors, bypassing the need for T-lymphocytic help and overcoming T-lymphocytic interference. Int J Cancer 1996; 67:142–7.
34. Tahara M, Pergolizzi RG, Kobayashi H, et al. Trans-splicing repair of CD40 ligand deficiency results in naturally regulated correction of a mouse model of hyper-IgM X-linked immunodeficiency. Nat Med 2004; 10:835–41.
35. Byrd L, Potter M, Mock B, Huppi K. The effect of the nude gene on plasmacytoma development in BALB/cAn mice. Curr Top Microbiol Immunol 1988;137:268–75.
36. Adams JM, Harris AW, Pinkert CA, et al. The c-*myc* oncogene driven by immunoglobulin enhancers induces lymphoid malignancy in transgenic mice. Nature 1985; 318:533–8.
37. Suda Y, Aizawa S, Hirai S, et al. Driven by the same Ig enhancer and SV40 T promoter ras induced lung adenomatous tumors, *myc* induced pre-B cell lymphomas and SV40 large T gene a variety of tumors in transgenic mice. EMBO J 1987;6:4055–65.
38. Schmidt EV, Pattengale PK, Weir L, Leder P. Transgenic mice bearing the human c-*myc* gene activated by an immunoglobulin enhancer: a pre-B-cell lymphoma model. Proc Natl Acad Sci U S A 1988;85: 6047–51.
39. Butzler C, Zou X, Popov AV, Bruggemann M. Rapid induction of B-cell lymphomas in mice carrying a human IgH/c-mycYAC. Oncogene 1997;14:1383–8.
40. Palomo C, Zou X, Nicholson IC, Butzler C, Bruggemann M. B-cell tumorigenesis in mice carrying a yeast artificial chromosome-based immunoglobulin heavy/c-*myc* translocus is independent of the heavy chain intron enhancer (Emu). Cancer Res 1999;59:5625–8.
41. Kovalchuk AL, Qi CF, Torrey TA, et al. Burkitt lymphoma in the mouse. J Exp Med 2000;192:1183–90.
42. Rosenbaum H, Harris AW, Bath ML, et al. An E mu-v-abl transgene elicits plasmacytomas in concert with an activated *myc* gene. EMBO J 1990;9:897–905.
43. Janz S, Potter M, Rabkin CS. Lymphoma- and leukemia-associated chromosomal translocations in healthy individuals. Genes Chromosomes Cancer 2003; 36:211–23.
44. Janz S, Müller J, Shaughnessy J, Potter M. Detection of recombinations between c-*myc* and immunoglobulin switch α in murine plasma cell tumors and preneoplastic lesions by polymerase chain reaction. Proc Natl Acad Sci U S A 1993;90:7361–5.
45. Nilsson JA, Cleveland JL. Myc pathways provoking cell suicide and cancer. Oncogene 2003;22:9007–21.
46. Felsher DW, Bishop JM. Reversible tumorigenesis by MYC in hematopoietic lineages. Mol Cell 1999;4:199–207.
47. Weber A, Liu J, Collins I, Levens D. TFIIH operates through an expanded proximal promoter to fine-tune c-*myc* expression. Mol Cell Biol 2005;25:147–61.
48. Levens DL. Reconstructing MYC. Genes Dev 2003;17: 1071–7.
49. Reimold AM, Iwakoshi NN, Manis J, et al. Plasma cell differentiation requires the transcription factor XBP-1. Nature 2001;412:300–7.
50. Lee AH, Iwakoshi NN, Anderson KC, Glimcher LH. Proteasome inhibitors disrupt the unfolded protein response in myeloma cells. Proc Natl Acad Sci U S A 2003;100:9946–51.
51. Lin Y, Wong K, Calame K. Repression of c-*myc* transcription by Blimp-1, an inducer of terminal B cell differentiation. Science 1997;276:596–9.

Insertion of *Myc* into *Igh* Accelerates Peritoneal Plasmacytomas in Mice

Sung Sup Park, Arthur L. Shaffer, Joong Su Kim, et al.

Cancer Res 2005;65:7644-7652.